ACS Biomaterials SCIENCE & ENGINEERING

pubs.acs.org/journal/abseba

Letter

Rapid Single-Step Growth of MOF Exoskeleton on Mammalian Cells for Enhanced Cytoprotection

Laura Ha, UnJin Ryu, Dong-Chang Kang, Jung-Kyun Kim, Dengrong Sun, Yong-Eun Kwon, Kyung Min Choi,* and Dong-Pyo Kim*

Cite This: https://doi.org/10.1021/acsbiomaterials.1c00539

Read Online

ACCESS | Metrics & More | Article Recommendations | Supporting Information

ABSTRACT: Mammalian cells are promising agents for cell therapy, diagnostics, and drug delivery. For full utilization of the cells, development of an exoskeleton may be beneficial to protecting the cells against the environmental stresses and cytotoxins to which they are susceptible. We report here a rapid single-step method for growing metal−organic framework (MOF) exoskeletons on a mammalian cell surface under cytocompatible conditions. The MOF exoskeleton coating on the mammalian cells was developed via a one-pot biomimetic mineralization process. With the exoskeleton on, the individual cells were successfully protected against cell protease (i.e., Proteinase K), whereas smaller-sized nutrient transport across the exoskeleton was maintained. Moreover, vital cellular activities mediated by transmembrane GLUT transporter proteins were also unaffected by the MOF exoskeleton formation on the cell surfaces. Altogether, this ability to control the access of specific molecules to a single cell through the porous exoskeleton, along with the cytoprotection provided, should be valuable for biomedical applications of mammalian cells.

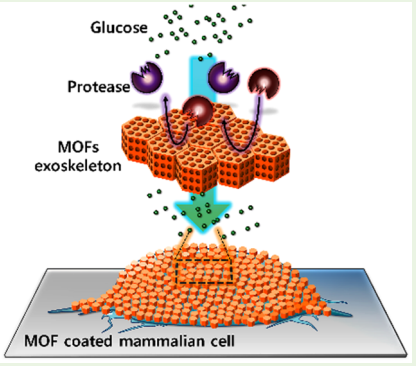

KEYWORDS: *artificial exoskeleton, biomimetic mineralization, cytoprotection, mammalian cell, metal−organic frameworks*

INTRODUCTION

Mammalian cells such as stem cells can be promising agents for cell therapy, diagnostics, and drug delivery.[1−3] However, because of the absence of a robust cell wall or exoskeleton, mammalian cells are sensitive to the subtle changes in their microenvironment such as osmotic pressure, nutrient level, and cytotoxins.[4] It is, therefore, necessary for full utilization of the mammalian cells that they are protected and their viabilities are assured.

The field of artificial cell coating with mechanically durable materials has matured rapidly since the pioneering work in the early 2000s. Although early research humbly began by coating dead cells, it quickly evolved into coating of individual living cells.[5−9] The synthetic strategies with various materials such as silicon dioxide, silicon dioxide-titanium dioxide, polydopamine, and iron-tannate coordination complex have been reported for the formation of cell-in-shell structures.[10−12] Interestingly, these coating processes have offered degree of cytoprotection against various stresses such as UV−C radiation, lyticase, and toxic nanoparticles. However, complicated and time-consuming multistep processes for cell coating and poor control of the permeability of the coating have also been identified as weaknesses of the systems.[13−15] Therefore, a simplified coating process would certainly be beneficial for reducing stress to the extremely labile mammalian cells.

Metal−organic frameworks (MOFs) are a class of porous materials that are constructed from metal nodes connected via organic linkers. Among them, zeolitic imidazolate frameworks (ZIFs), which consist of metal ions bridged tetrahedrally by imidazolate-type linkers, are often addressed in encapsulating various biomolecules such as proteins, insulin, and DNA because of its well-known biocompatibility, exceptional chemical stability, and the potential to be synthesized in pure water conditions. Another beneficial feature of ZIF is its high porosity; the highly porous property of ZIF allows delivery of small-sized molecules such as nutrients from the external environment to the encapsulated biomolecules through the microsized pores.[16−24] Thus, recently, the concept has been extended from their use as matrices for encapsulating biomolecules to more complex systems like mammalian cells. For example, Zhu et al. have reported a cell-in-shell structure by linking separately synthesized ZIF nanoparticles (ZIF NP) onto the individual mammalian cell surface assisted by tannic acid as a chemical binder.[13] Although ZIF NP-coated cells successfully demonstrated good cell viability under the stressful conditions, the tannic acid treatment still induce stress on the

Received: April 21, 2021
Accepted: June 10, 2021

cell and can possibly deteriorate the intrinsic porous properties of the MOF shell.[25,26]

An alternative approach to develop a MOF-coated cell is via biomimetic mineralization.[27] In this method, nucleation and growth of the MOF precursors are facilitated by a biomolecule-rich cell membrane; and cell coating is achieved in a rapid, single-step and binder-free manner. Thus, herein, we demonstrated the formation of protective ZIF-8 shell on individual human breast cancer cells (MDA-MB-231) as an artificial exoskeleton applying biomimetic mineralization approach. The well-known stability and biocompatibility of ZIF coating layer must protect the mammalian cells to enhance the tolerance in cytotoxic enzyme presenting environments. Furthermore, the highly porous nature of the ZIF layer allows the transport of small essential nutrients like glucose from its environment to the cells without disrupting the intrinsic function of transmembrane protein such as GLUT transporter (Scheme 1). The formation of ZIF-based artificial exoskeleton

Scheme 1. Schematic Illustration of Formation of MOF Exoskeleton[a]

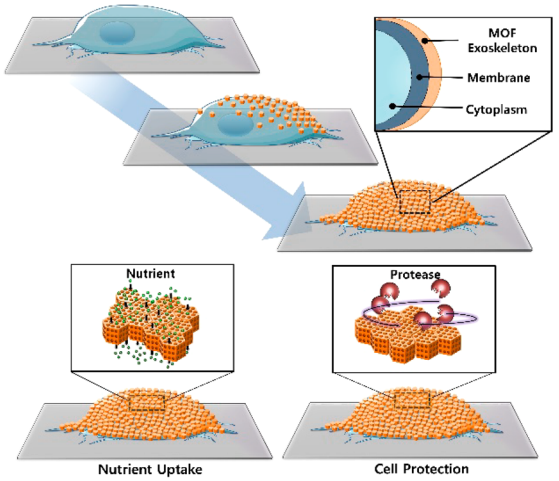

[a]Nutrients such as glucose can pass through the exoskeleton, whereas cytotoxins cannot.

on the mammalian cell will certainly be beneficial not only for the safe handling of the cells but also for biomedical applications.

RESULTS AND DISCUSSION

Synthesis of MOF Nanoparticles in Phosphate Buffer Saline and Validation of Stability in Cell Culture Media. Typically, the biomimetic mineralization method for biomolecule encapsulation is performed via one-pot synthesis, whereas biomolecules such as proteins are dispersed in deionized (DI) water with MOF precursors.[27] However, unfortunately, the reported DI water-based coating method with MOF precursors is not suitable to apply in mammalian cell coating because the process-driven osmotic pressure induces mammalian cell rupture.[10] Therefore, development of a new protocol is highly demanded for MOF synthesis on the mammalian cells in cytocompatible conditions.

In light of this issue, we chose 1× PBS (phosphor buffer saline), one of the most commonly used cytocompatible solvents, to examine the synthesis of ZIF-8. Initially, zinc acetate dehydrate ($Zn(OAc)_2{\cdot}2H_2O$) and 2-methylimidazole (Hmim) were separately prepared in 1× PBS solution. The milky solution was perceived instantly after equal volumes of the two solutions were poured and stirred at room temperature. The collected products were compared structurally with the reported ZIF-8 as formed in DI water condition by analyzing powder X-ray diffraction (PXRD) in the presence of commercial TiO_2 (anatase) as an internal standard, scanning electron microscopy (SEM), and Brunauer–Emmett–Teller (BET) measurements.

The sharp XRD pattern that represented the high crystallinity of the product were observed after 5 min synthesis of ZIF-8 in 1× PBS solution; the intensity of the peak increased with increasing synthesis time (Figure 1A). The

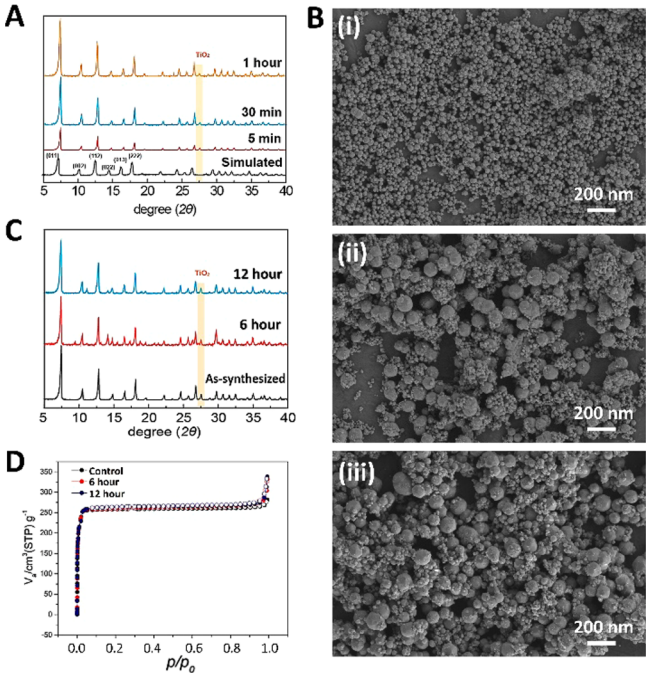

Figure 1. Characterization of ZIF-8 nanoparticles synthesized in 1× PBS. (A) XRD patterns of ZIF-8 nanoparticles synthesized in 1× PBS for 5 min, 30 min, and 1 h. (B) High-resolution SEM images of ZIF-8 nanoparticles in 1× PBS for (i) 5 min, (ii) 30 min, and (iii) 1 h (Bar: 200 nm). (C) XRD patterns of the ZIF-8 nanoparticles incubated in cell culture media for 6 and 12 h. (D) BET patterns of ZIF-8 nanoparticles incubated in cell culture media for 0, 6, and 12 h.

SEM images in Figure 2B and Figure S1 show the unique morphology of the particles with no discernible difference. The average particle size gradually increased with longer synthesis time as expected, approximately 140 nm for 5 min, 280 nm for 30 min, and 320 nm for 5 min, 30 min, and 1 h of synthesis, respectively. N_2 adsorption–desorption isotherms of ZIF-8 product exhibited a type I branches (Figure S2A). The BET surface area (S_{BET}) and micropore volume were calculated to be 1061 m^2/g and 0.27 cm^3/g, respectively. These results signifies that the overall structure of the synthesized ZIF-8 crystals is nearly analogous to the structure of standard ZIF-8 that was synthesized in DI water.[28] In addition, the size-dependent permeability of ZIF-8 was verified using molecular dyes of different sizes (Figure S2B, C).

As we are interested in applying ZIF-8 as an individual cell exoskeletal coating material, the structural stability of the synthesized ZIF-8 in cell culture media is significant. Upon suspending the as-synthesized samples in cell culture media,

https://doi.org/10.1021/acsbiomaterials.1c00539
ACS Biomater. Sci. Eng. XXXX, XXX, XXX–XXX

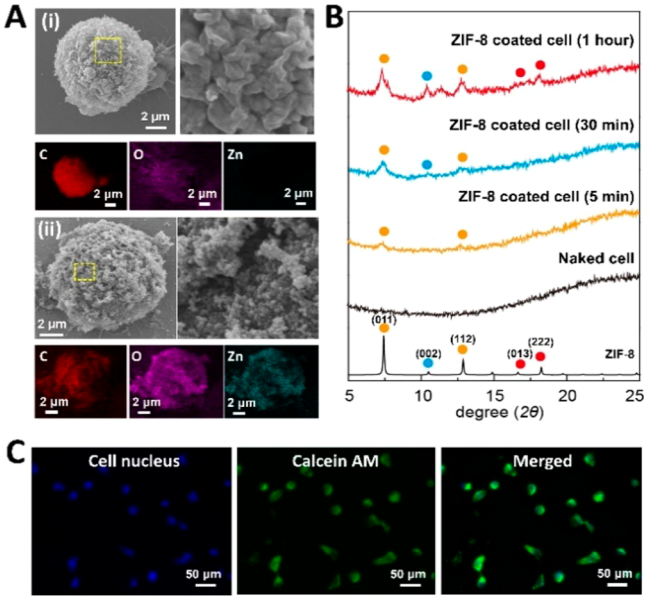

Figure 2. Development of ZIF-8-coated MDA-MB-231 cells. (A) SEM imaging and EDS elemental mapping analyses of (i) naked cell surface, and (ii) ZIF-8 exoskeleton grown cell surface (bar: 2 μm). (B) XRD patterns of standard ZIF-8 crystals and ZIF-coated cells after 5 min, 30 min, and 1 h. (C) Cell viability upon ZIF-8 coating (bar: 50 μm).

Dulbecco's modified Eagle's medium (DMEM), the structural integrity was monitored by PXRD and N_2 sorption. Figure 1C demonstrates that the normalized intensity of the peak arising from the (011) plane of ZIF-8 crystal remained unchanged with an incubation time of up to 12 h. In addition, no detectable change in nitrogen sorption was observed in ZIF-8 crystals before and after the incubation in DMEM, which indicates that all ZIF-8 samples remained intact in DMEM (Figure 1D).

Rapid Single-Step Synthesis of MOF Exoskeleton on Mammalian Cells. The successful synthesis of the ZIF-8 in 1× PBS solution prompted us to apply the protocol to the formation of exoskeleton on mammalian cells. Previous studies have shown that chemical functional groups such as −COOH, −OH, and $-NH_2$ can promote the formation of a MOF thin film on the substrate by anchoring the metal and organic linkers and nucleating the growth of the MOFs on the substrate.[29] Indeed, because of the presence of biomolecules (i.e., proteins) mammalian cell membranes are well covered with the above functional groups.[30] Therefore, biomimetic mineralization of ZIF-8 occurs on the biomolecule-rich and negatively charged mammalian cell membrane by attraction and concentration of positively charged zinc ions around the cell surface and subsequent crystallization of MOF crystals.[27,31,32] The ZIF-8-coated mammalian cells were produced by incubating the glass adhered MDA-MB-231 cell-line in a 1× PBS solution containing $Zn(OAc)_2{\cdot}2H_2O$ and Hmim with gentle shaking. After 5 min of incubation at room temperature, the cells were separated from the solution and washed with DMEM three times. Figure 2A shows the morphology and elemental distribution of the ZIF-8 exoskeleton covering the MDA-MB-231 cells using SEM and energy-dispersive X-ray spectroscopy (EDS). SEM micrographs revealed that the exposed surface of individual cells was well-covered by layers of ZIF-8. Elemental mapping confirmed an uniform distribution of overlapping signals corresponding to O (From the MDA-MB-231 cells), C (from the MDA-MB-231 cells and ZIF-8), and Zn (from the ZIF-8). Subsequently, we performed XRD analysis of the coating to confirm the presence of ZIF-8 particles on the cultured MDA-MB-231 cells with more than 80% confluences on the glass substrate. The diffraction pattern of ZIF-8-coated cells were examined Figure 2B. When the cells were grown for 5 min in the ZIF precursor solution, the data show the characteristic (011) and (112) peaks of the ZIF-8 crystal peaks with weak intensity, presumably due to the thin thickness of ZIF nanoparticles on the surfaces of MDA-MB-231 cells. Along the extended coating time, however, the diffraction pattern of ZIF-8-coated cells demonstrates the gradually increased intensity of the (011) and (112) peaks of the ZIF-8 crystal; in addition, the characteristic peaks of ZIF-8, including (002), (013), and (222), began to appear. TEM analysis was further performed to examine the thickness of ZIF-8 layer covering a single cell surface. On the basis of the TEM data, the thickness of the coating layer on the cell surface varied approximately ranging from 50 to 400 nm (Figure S3). This wide thickness distribution is often observed owing to uneven ZIF nucleation and growth.[33,34] Next, cell viability assay was performed with Calcein AM to examine the effect of ZIF-8 coating on the MDA-MB-231 cell viability. Calcein AM is a cell permeant fluorescent dye that emits fluorescence when digested by esterase, which is present in healthy live cells.[35] As seen in Figure 2C and Figure S4A, a bright fluoresce signal was observed in ZIF-8-coated cells after the ZIF-8 coating process for 5 min. Note that, ZIF-8-coated cells maintained viability for 72 h (Figure S4B). Interestingly, unlike the native cells, which multiply rapidly and proliferate for 72 h, ZIF-8-coated cells exhibited arrested replication behavior, as shown in Figure S4C. Hence, we carefully predict that MOF-coated cells entered into a dormant state.

In addition, comparisons are made between the native MDA-MB-231 cells and MDA-MB-231 cells coated with ZIF-8 on the entire surface for the cell-microenvironment attachment. The native MDA-MB-231 cells adhered well to the ECM-coated substrate, whereas the cells completely coated with ZIF-8 hardly adhere to the substrate (Figure S4D). However, after removing the ZIF-8 layer, the substrate-unbound cells began to adhere to the substrate with good cell viability as analyzed with Calcein AM (Figure S4E).

Validation of Cytoprotective Role of MOF Coating. As successful formation of an exoskeleton layer around the cells is achieved, the armed protection potential of the ZIF-8-coated MDA-MB-231 cells in toxic condition is investigated under the simulated unpleasant environments in the presence of Proteinase K (M_w = 28.9 kDa), a nonspecific serine protease that digests the cell surface proteins and deters the cell adhesion.[36,37] Note that, Proteinase K is selected as model cytotoxin as it has similar size as antibodies.[38,39] When the naked cells and the ZIF-8-coated cells were separately cultured in the cell culture media containing Proteinase K, cell adhesion behaviors were examined with an optical microscope for an hour. In general, dramatic change of the morphology and surface adhesion were observed in the naked cells that started to round up and lost cell attachment on the glass substrate within 30 min, which was a notably contrasting feature from the ZIF-8-coated cells that did not show significant changes (Figure 3A). For the quantitative analysis, the cell attachment is measured by calculating the percent area of cell coverage using an *ImageJ* software. Figure 3B shows that there was a

https://doi.org/10.1021/acsbiomaterials.1c00539
ACS Biomater. Sci. Eng. XXXX, XXX, XXX−XXX

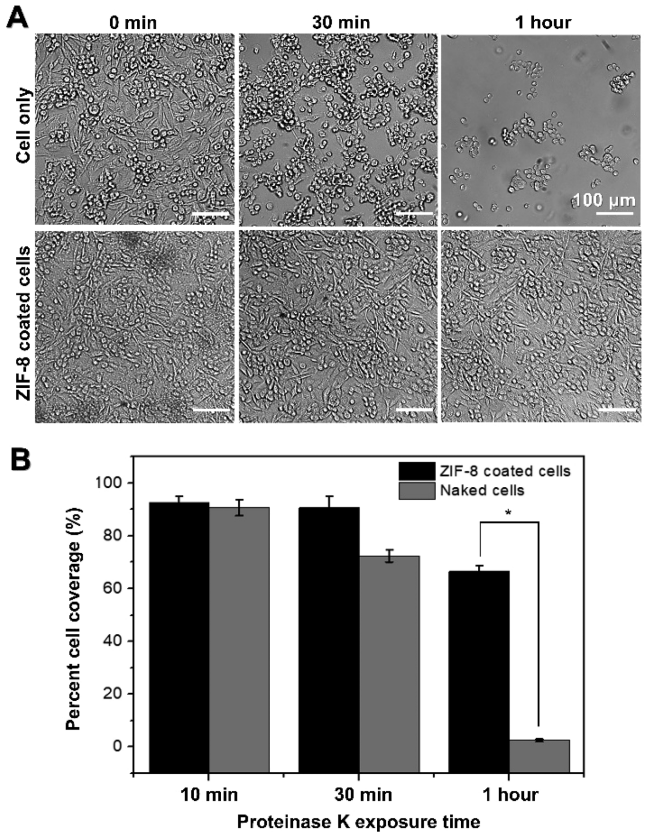

Figure 3. Enhanced cytoprotective performance of ZIF-8-coated cell compared to the naked cell in the presence of Proteinase K. (A) Bright-field images of cell attachment, treated with Proteinase K (bar: 100 μm). (B) Quantitative analysis of cell coverage on the surfaces (*$P < 0.05$).

little difference in the percent cell coverage between the naked and the coated cells at the early stage of 10 min of exposure of Protease K. As time passes on, however, the difference becomes more evident. A marked difference in the cell coverage was observed after 60 min: only 3% for the naked cells versus 66.5% for the ZIF-8-coated cells. Altogether, these results validate the enhanced cytoprotective function of ZIF-8 layer against the cytotoxic enzyme. The results also infer that the large-size Proteinase K is unable to penetrate into the microporous ZIF-8 exoskeletal layer, thus, failing to digest the cells. In addition, we compared the cytoprotective performances of our biomimetic mineralization method to that of the tannic acid-assisted ZIF-8 nanoparticle (ZIF-8/TA) coating method as lately reported.[13] Interestingly, after 1 h of incubation under the Proteinase K presenting environment, a greater amount of the ZIF-8/TA-coated cells disappeared, as shown in Figure S5.

Nutrient Permeability through MOF Exoskeleton. For the protected cells to be useful, they must be able to take up nutrients and signaling molecules from the microenvironment to survive. Thus, we attempt to verify whether the exoskeletal layer interfere the D-glucose uptake behavior by mammalian cells. D-Glucose is an essential source of energy for cell survival and growth, thus transport of the glucose molecules through the exoskeletal layer is essential.[40] Hence, we primarily examined the D-glucose permeability of ZIF-8 via confocal microscopy. The D-glucose permeability into ZIF-8 particle itself was visualized by soaking a large-sized single crystal ZIF-8 (sc-ZIF-8) in ethanol solution containing 0.5 mM fluorescent D-glucose analog, 2-[N-(7-nitrobenz-2-oxa-1,3-diazol-4-yl) amino]-2-deoxy-D-glucose (2-NBDG), for 1 day. As shown in Figure S6, the confocal Z-stacking images clearly illustrates that 2-NBDG is inserted into the entire area from the surface to the center of the ZIF-8 crystal. Furthermore, the D-glucose loading and releasing behavior of ZIF-8 was quantitatively analyzed by nuclear magnetic resonance (^{1}H NMR) measurement. The glucose was loaded by simply soaking ZIF-8 particles in 1.25 mM glucose deuterium oxide (D_2O) solution for 1 day. Consecutively, the glucose amount from the ZIF-8 was released by placing to pure D_2O and calculated using a standard curve (R^2 = 0.99977, Figure S7). As shown in Figure 4A and Figure S8, 6 μmol kg^{-1} D-glucose was loaded into ZIF-

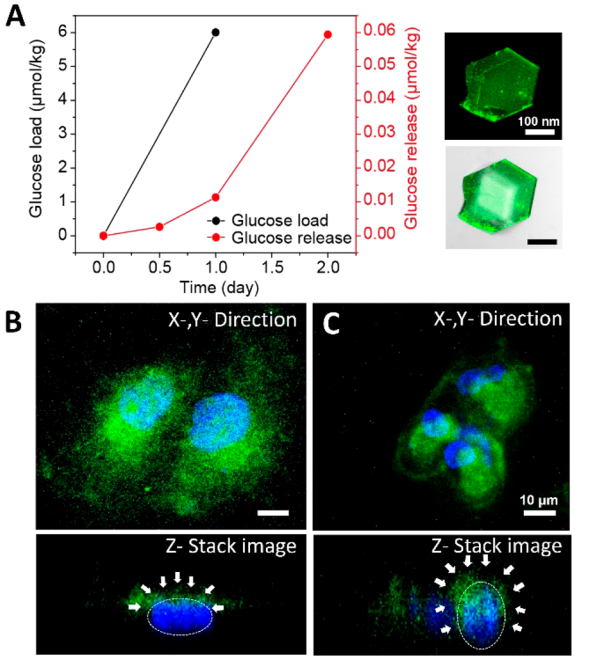

Figure 4. D-Glucose permeability through the ZIF-8 exoskeleton layer. (A) $_1$H NMR-based glucose load/release trend and confocal microscope image of 2-NBDG-loaded ZIF-8 particle (bar: 100 nm). (B) Z-stacked confocal microscope images of ZIF-8-coated cells before incubation (blue, cell nucleus; green, 2-NBDG; bar, 10 μm). (C) Z-stacked confocal microscope images of ZIF-8-coated cells after 1 h of incubation (blue, cell nucleus; green, 2-NBDG; bar, 10 μm).

8 within 1 day; and 0.0026, 0.0114, and 0.0594 μmol kg^{-1} D-glucose was released from the ZIF-8 after 12, 24, and 48 h in pure D_2O, respectively. Although relatively fast glucose loading into the ZIF-8 nanoparticles was observed, the release of the glucose was about 100 times slower than loading.[41]

Validation of Preserved Function of GLUT Transported for Nutrient Transport into the Cells. Generally, D-glucose uptake by the mammalian cells is mediated by the active transmembrane protein called GLUT transporter rather than passive diffusion.[42,43] Thus, for the successful transport of D-glucose into the cell, the activities of GLUT transporters on the cell membrane are critical. To verify the uptake, we placed ZIF-8-coated MDA-MB-231 cells in the 2-NBDG containing cell culture media for 5 min. After sequential intensive washing with DMEM to remove surface adsorbed 2-NBDG as much as possible, glucose-depleted cell culture media was added and incubated in 37 °C for 1 h. On the basis of confocal

https://doi.org/10.1021/acsbiomaterials.1c00539
ACS Biomater. Sci. Eng. XXXX, XXX, XXX−XXX

micrographs, 2-NBDG molecules on the apical part of the cell were examined at 0 min incubation (Figure 4B; Figure S9). After an hour of incubation, green fluorescence coming from 2-NBDG was observed in the cell cytoplasm as well as at the apical layer of cells (Figure 4C). Altogether, we could confirm that ZIF material can act as a bioactive porous layer that not only permit the diffusion of small essential nutrients like glucose from its environment to the cells but also allow the active function of transmembrane protein, GLUT transporter. We believe that this result envisions the controlled access of specific molecules to the single cell level through a porous artificial exoskeleton to mediate the intrinsic behavior of various transmembrane proteins, which is useful for cell biological applications.

Development of MOF-Janus Cells for Potential Drug Delivery Application. Significant efforts have been made over the decades to develop the novel drug delivery systems using the living cells.[44,45] More recently, the Janus design, which asymmetrically decorates the cell surface with therapeutic drugs, has been reported with enhanced drug delivery efficiency.[46,47] Thus, as a proof-of-concept, we tried to develop MOF-Janus cells by asymmetrically coating the MOF layer with therapeutic agent to the MDA-MB-231 cells. Note that we selected fluorescent labeled bovine serum albumin (FITC-BSA) as a model drug. Briefly, MOF-Janus cells were attained by (1) coating the substrate adhering MDA-MB-231 cells with FITC-BSA, $Zn(OAc)_2{\cdot}2H_2O$, and Hmim in 1× PBS and (2) subsequently releasing the cells from the substrate using enzyme trypsin. As shown in Figure 5A, asymmetrical

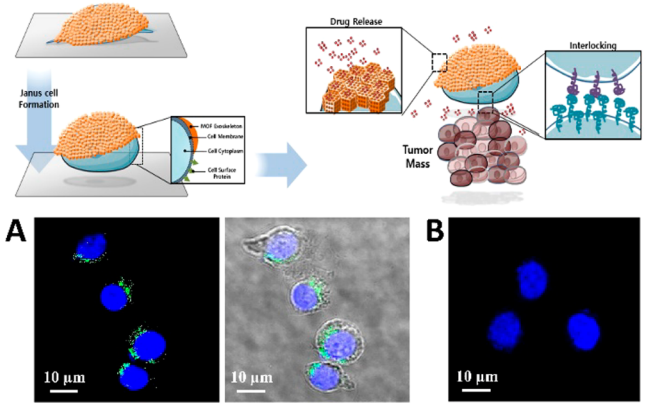

Figure 5. Proof-of-concept demonstration of MOF-Janus cells. Confocal micrograph images of (A) FITC-BSA-loaded MOF-Janus cells, and (B) pH-responsive release of FITC-BSA from the MOF-Janus cells at pH 6 (blue, cell nucleus; green, FITC-BSA; bar, 10 μm).

loadings of FITC-BSA on the MOF-Janus cells were examined. Furthermore, release of encapsulated FITC-BSA was observed when the MOF-Janus cells are placed in acidic culture media at pH 6 for 1 h (Figure 5B). The release of the FITC-BSA was confirmed as disappearance of the green fluorescence from the Janus cell; no change in cell nucleus morphology was examined. Lastly, the viability of the Janus cells after BSA release was examined. About 79% of Janus cells were viable after release of the FITC-BSA (Figure S10).

CONCLUSIONS

We have presented a novel rapid single formation of highly porous ZIF-8 on individual living mammalian cells under cytocompatible conditions in 1× PBS as the solvent system. This simple one-step approach enables one to coat a biocompatible and mechanically durable artificial exoskeleton on the surface of human cell-line, demonstrating a superior cytoprotective performance that enhances cell survival. Moreover, the ZIF-8 exoskeleton layer acts not only as a bioactive porous layer that allows uptake of small glucose nutrient by the mammalian cells but also act as a physical barrier that protects the cells against cell toxic protease such as Proteinase K. Our rapid one-pot approach for cytoprotective MOF formation allows facile single cell packaging technology with no need of sophisticated technique or special equipment. Hence, our facile approach is applicable for mass production of a highly uniform MOF-coated single cell, although further research is required to meet industrial or clinical demands in depth. Altogether, these results bode well for the potential use of multifunctional MOF coatings on viable mammalian cells for various biomedical applications with the promoted tolerance in cell handling.

ASSOCIATED CONTENT

Supporting Information

The Supporting Information is available free of charge at https://pubs.acs.org/doi/10.1021/acsbiomaterials.1c00539.

Materials and methods information on ZIF-8 synthesis, cell culture, ZIF-8 coating on living cells, XRD, SEM, TEM confocal micrograph characterizations of ZIF-8 coating on living cells, cell viability assays, statistical methods; Figure S1 showing scanning electron microscopy (SEM/EDS) image of synthesized ZIF-8 nanoparticles in 1× PBS solution, Figure S2 for nitrogen adsorption isotherm and small molecule permeability of as-synthesized ZIF-8 nanocrystals, Figure S3 for TEM micrograph image of ZIF-8-coated cells, Figure S4 showing intermediate to long-term cell viability after ZIF-8 exoskeleton formation on cells and their intermediate to long-term viabilities, Figure S5 for cell protection against cytotoxic proteins, Figures S6−S9 for analysis of glucose permeability though the ZIF-8 exoskeleton analysis, and Figure S10 for Janus cell viability after drug release (PDF)

AUTHOR INFORMATION

Corresponding Authors

Dong-Pyo Kim − *Center for Intelligent Microprocess of Pharmaceutical Synthesis Department of Chemical Engineering, Pohang University of Science and Technology (POSTECH), Pohang 37673, Republic of Korea;* orcid.org/0000-0003-4676-9766; Email: dpkim@postech.ac.kr

Kyung Min Choi − *Department of Chemical and Biological Engineering and Institute of Advanced Materials & Systems, Sookmyung Women's University, Seoul 04310, Republic of Korea*; Email: kmchoi@sm.ac.kr

Authors

Laura Ha − *Center for Intelligent Microprocess of Pharmaceutical Synthesis Department of Chemical Engineering, Pohang University of Science and Technology (POSTECH), Pohang 37673, Republic of Korea*

UnJin Ryu − *Department of Chemical and Biological Engineering and Institute of Advanced Materials & Systems,*

https://doi.org/10.1021/acsbiomaterials.1c00539
ACS Biomater. Sci. Eng. XXXX, XXX, XXX−XXX

Sookmyung Women's University, Seoul 04310, Republic of Korea; Present Address: Department of Chemical and Biological Engineering and Industry Collaboration Center, Sookmyung Women's University, Cheongpa-ro 47-gil 100, Yongsan-gu, Seoul, 04310, Republic of Korea; orcid.org/0000-0002-4854-3587

Dong-Chang Kang − *Center for Intelligent Microprocess of Pharmaceutical Synthesis Department of Chemical Engineering, Pohang University of Science and Technology (POSTECH), Pohang 37673, Republic of Korea*

Jung-Kyun Kim − *Center for Intelligent Microprocess of Pharmaceutical Synthesis Department of Chemical Engineering, Pohang University of Science and Technology (POSTECH), Pohang 37673, Republic of Korea*

Dengrong Sun − *Center for Intelligent Microprocess of Pharmaceutical Synthesis Department of Chemical Engineering, Pohang University of Science and Technology (POSTECH), Pohang 37673, Republic of Korea*

Yong-Eun Kwon − *Center for Scientific Instrumentation, Korea Basic Science Institute (KBSI), Daejeon 34133, Republic of Korea*

Complete contact information is available at: https://pubs.acs.org/10.1021/acsbiomaterials.1c00539

Author Contributions

The manuscript was written through contributions of all authors. All authors have given approval to the final version of the manuscript. L.H. and U.R. contributed equally. K.M.C. and D.-P.K. contributed equally in this work.

Notes

The authors declare no competing financial interest.

■ ACKNOWLEDGMENTS

This work was supported by the National Research Foundation of Korea (NRF) grant funded by the Korean government (MSIT) (NRF-2017R1A3B1023598 & NRF-2019R1A2C4069764).

■ REFERENCES

(1) Yoo, J.-W.; Irvine, D. J.; Discher, D. E.; Mitragotri, S. Bio-inspired, bioengineered and biomimetic drug delivery carriers. *Nat. Rev. Drug Discovery* **2011**, *10*, 521−535.

(2) Naldini, L. Ex vivo gene transfer and correction for cell-based therapies. *Nat. Rev. Genet.* **2011**, *12*, 301−315.

(3) Stewart, M. P.; Sharei, A.; Ding, X.; Sahay, G.; Langer, R.; Jensen, K. F. In vitro and ex vivo strategies for intracellular delivery. *Nature* **2016**, *538*, 183−192.

(4) Riccò, R.; Liang, W.; Li, S.; Gassensmith, J. J.; Caruso, F.; Doonan, C.; Falcaro, P. Metal-Organic Frameworks for Cell and Virus Biology: A Perspective. *ACS Nano* **2018**, *12*, 13−23.

(5) Hong, D.; Park, M.; Yang, S. H.; Lee, J.; Kim, Y.-G.; Choi, I. S. Artificial spores: cytoprotective nanoencapsulation of living cells. *Trends Biotechnol.* **2013**, *31*, 442−447.

(6) Diaspro, A.; Silvano, D.; Krol, S.; Cavalleri, O.; Gliozzi, A. Single Living cell encapsulation in nano-organized polyelectrolyte shells. *Langmuir* **2002**, *18*, 5047−5050.

(7) Fakhrullin, R. F.; Lvov, Y. M. "Face-lifting" and "make-up" for microorganisms: layer-by-layer polyelectrolyte nanocoating. *ACS Nano* **2012**, *6*, 4557−4564.

(8) Kozlovskaya, V.; Harbaugh, S.; Drachuk, I.; Shchepelina, O.; Kelley-Loughnane, N.; Stone, M.; Tsukruk, V. V. Hydrogen-bonded LbL shells for living cell surface engineering. *Soft Matter* **2011**, *7*, 2364−2372.

(9) Drachuk, I.; Gupta, M. K.; Tsukruk, V. V. Biomimetic Coatings to Control Cellular Function through Cell Surface Engineering. *Adv. Funct. Mater.* **2013**, *23*, 4437−4453.

(10) Park, J. H.; Hong, D.; Lee, J.; Choi, I. S. Cell-in-Shell Hybrids: Chemical Nanoencapsulation of Individual Cells. *Acc. Chem. Res.* **2016**, *49*, 792−800.

(11) Drachuk, I.; Shchepelina, O.; Lisunova, M.; Harbaugh, S.; Kelley-Loughnane, N.; Stone, M.; Tsukruk, V. V. pH-Responsive Layer-by-Layer Nanoshells for Direct Regulation of Cell Activity. *ACS Nano* **2012**, *6*, 4266−4278.

(12) Youn, W.; Ko, E. H.; Kim, M.-H.; Park, M.; Hong, D.; Seisenbaeva, G. A.; Kessler, V. G.; Choi, I. S. Cytoprotective Encapsulation of Individual Jurkat T Cells within Durable TiO2 Shells for T-Cell Therapy. *Angew. Chem.* **2017**, *129*, 10842−10846.

(13) Zhu, W.; Guo, J.; Amini, S.; Ju, Y.; Agola, J. O.; Zimpel, A.; Shang, J.; Noureddine, A.; Caruso, F.; Wuttke, S.; Croissant, J. G.; Brinker, C. J. SupraCells: Living Mammalian Cells Protected within Functional Modular Nanoparticle-Based Exoskeletons. *Adv. Mater.* **2019**, *31*, 1900545.

(14) Kadowaki, K.; Matsusaki, M.; Akashi, M. Control of Cell Surface and Functions by Layer-by-Layer Nanofilms. *Langmuir* **2010**, *26*, 5670−5678.

(15) Oliveira, M. B.; Hatami, J.; Mano, J. F. Coating Strategies Using Layer-by-layer Deposition for Cell Encapsulation. *Chem. - Asian J.* **2016**, *11*, 1753−1764.

(16) Furukawa, H.; Cordova, K. E.; O'keeffe, M.; Yaghi, O. M. The chemistry and applications of metal-organic frameworks. *Science* **2013**, *341*, 1230444.

(17) Wu, H.; Zhou, W.; Yildirim, T. Hydrogen Storage in a Prototypical Zeolitic Imidazolate Framework-8. *J. Am. Chem. Soc.* **2007**, *129*, 5314−5315.

(18) Hayashi, H.; Côté, A. P.; Furukawa, H.; O'Keeffe, M.; Yaghi, O. M. Zeolite A imidazolate frameworks. *Nat. Mater.* **2007**, *6*, 501−506.

(19) Banerjee, R.; Furukawa, H.; Britt, D.; Knobler, C.; O'Keeffe, M.; Yaghi, O. M. Control of Pore Size and Functionality in Isoreticular Zeolitic Imidazolate Frameworks and their Carbon Dioxide Selective Capture Properties. *J. Am. Chem. Soc.* **2009**, *131*, 3875−3877.

(20) Liang, K.; Ricco, R C. M.; Doherty, C. M.; Styles, M. J.; Bell, S.; Kirby, N.; Mudie, S.; Haylock, D.; Hill, A. J.; Doonan, C. J.; Falcaro, P. Biomimetic mineralization of metal-organic frameworks as protective coatings for biomacromolecules. *Nat. Commun.* **2015**, *6*, 7240.

(21) Liang, K.; Carbonell, C.; Styles, M. J.; Ricco, R.; Cui, J.; Richardson, J. J.; Maspoch, D.; Caruso, F.; Falcaro, P. Biomimetic Replication of Microscopic Metal−Organic Framework Patterns Using Printed Protein Patterns. *Adv. Mater.* **2015**, *27*, 7293−7298.

(22) Liang, K.; Coghlan, C. J.; Bell, S. G.; Doonan, C.; Falcaro, P. Enzyme encapsulation in zeolitic imidazolate frameworks: a comparison between controlled co-precipitation and biomimetic mineralisation. *Chem. Commun.* **2016**, *52*, 473−476.

(23) Park, K. S.; Ni, Z.; Côté, A. P.; Choi, J. Y.; Huang, R.; Uribe-Romo, F. J.; Chae, H. K.; O'Keeffe, M.; Yaghi, O. M. Exceptional chemical and thermal stability of zeolitic imidazolate frameworks. *Proc. Natl. Acad. Sci. U. S. A.* **2006**, *103*, 10186−10191.

(24) Feng, S.; Zhang, X.; Shi, D.; Wang, Z. Zeolitic imidazolate framework-8 (ZIF-8) for drug delivery: a critical review. *Front. Chem. Sci. Eng.* **2021**, *15*, 221−237.

(25) Ge, X.; Li, C.; Li, Z.; Yin, L. Tannic acid tuned metal-organic framework as a high-efficiency chemical anchor of polysulfide for lithium-sulfur batteries. *Electrochim. Acta* **2018**, *281*, 700−709.

(26) Zhang, J.; Chen, D.; Han, D.; Cheng, Y.; Dai, C.; Wu, X.; Che, F.; Heng, X. Tannic acid mediated induction of apoptosis in human glioma Hs 683 cells. *Oncol. Lett.* **2018**, *15*, 6845−6850.

(27) Liang, K.; Ricco, R.; Doherty, C. M.; Styles, M. J.; Falcaro, P. Amino acids as biomimetic crystallization agents for the synthesis of ZIF-8 particles. *CrystEngComm* **2016**, *18*, 4264−4267.

(28) Pan, Y.; Liu, Y.; Zeng, G.; Zhao, L.; Lai, Z. Rapid synthesis of zeolitic imidazolate framework-8 (ZIF-8) nanocrystals in an aqueous system. *Chem. Commun.* **2011**, *47*, 2071−2073.
(29) Liu, J.; Woll, C. Surface-supported metal−organic framework thin films: fabrication methods, applications, and challenges. *Chem. Soc. Rev.* **2017**, *46*, 5730−5770.
(30) Lee, D. Y.; Cha, B.-H.; Jung, M.; Kim, A. S.; Bull, D. A.; Won, Y.-W. Cell surface engineering and application in cell delivery to heart diseases. *J. Biol. Eng.* **2018**, *12*, 28.
(31) Liang, K.; Richardson, J. J.; Cui, J.; Caruso, F.; Doonan, C. J.; Falcaro, P. Metal-organic framework coating as cytoprotective exoskeletons for living cells. *Adv. Mater.* **2016**, *28*, 7910−7914.
(32) Liang, K.; Richardson, J. J.; Doonan, C. J.; Mulet, X.; Ju, Y.; Cui, J. W.; Caruso, F.; Falcaro, P. An Enzyme-Coated Metal-Organic Framework Shell for Synthetically Adaptive Cell Survival. *Angew. Chem., Int. Ed.* **2017**, *56*, 8510−8515.
(33) Jeong, G.-Y.; Ricco, R.; Liang, K.; Ludwig, J.; Kim, J.-O.; Falcaro, P.; Kim, D.-P. Bioactive MIL-88A Framework Hollow Spheres via Interfacial Reaction In-Droplet Microfluidics for Enzyme and Nanoparticle Encapsulation. *Chem. Mater.* **2015**, *27*, 7903−7909.
(34) Faustini, M.; Kim, J.; Jeong, G.-Y.; Kim, J. Y.; Moon, H. R.; Ahn, W.-S.; Kim, D.-P. Microfluidic approach toward continuous and ultrafast synthesis of metal-organic framework crystals and hetero structures in confined microdroplets. *J. Am. Chem. Soc.* **2013**, *135*, 14619−14626.
(35) Neri, S.; Mariani, E.; Meneghetti, A.; Cattini, L.; Facchini, A. Calcein-acetyoxymethyl cytotoxicity assay: standardization of a method allowing additional analyses on recovered effector cells and supernatants. *Clin. Diagn. Lab. Immunol.* **2001**, *8*, 1131−1131.
(36) Tarone, G.; Galetto, G.; Prat, M.; Comoglio, P. M. Cell surface molecules and fibronectin-mediated cell adhesion: effect of proteolytic digestion of membrane proteins. *J. Cell Biol.* **1982**, *94*, 179−186.
(37) Vit, O.; Petrak, J. Integral membrane proteins in proteomics. How to break open the black box? *J. Proteomics* **2017**, *153*, 8−20.
(38) Larkin, J.; Henley, R. V.; Muthukumar, M.; Rosenstein, J. K.; Wanunu, M. High-Bandwidth Protein Analysis Using Solid-State Nanopores. *Biophys. J.* **2014**, *106*, 696−704.
(39) Reth, M. Matching Cellular Dimensions with Molecular Sizes. *Nat. Immunol.* **2013**, *14*, 765−767.
(40) Heywood, H. K.; Bader, D. L.; Lee, D. A. Glucose concentration and medium volume influence cell viability and glycosaminoglycan synthesis in chondrocyte-seeded alginate constructs. *Tissue Eng.* **2006**, *12*, 3487−3496.
(41) Han, Y.; Liu, W.; Huang, J.; Qiu, S.; Zhong, H.; Liu, D.; Liu, J. Cyclodextrin-Based Metal-Organic Frameworks (CD-MOFs) in Pharmaceutics and Biomedicine. *Pharmaceutics* **2018**, *10*, 271.
(42) Galochkina, T.; Ng Fuk Chong, M.; Challali, L.; Abbar, S.; Etchebest, C. New insights into GluT1 mechanics during glucose transfer. *Sci. Rep.* **2019**, *9*, 998.
(43) Szablewski, L. Expression of glucose transporters in cancers. *Biochim. Biophys. Acta, Rev. Cancer* **2013**, *1835*, 164−169.
(44) Chambers, E.; Mitragotri, S. Prolonged circulation of large polymeric nanoparticles by non-covalent adsorption on erythrocytes. *J. Controlled Release* **2004**, *100*, 111−119.
(45) Chambers, E.; Mitragotri, S. Long circulating nanoparticles via adhesion on red blood cells: mechanism and extended circulation. *Exp. Biol. Med. (London. U. K.)* **2007**, *232*, 958−966.
(46) Tang, S.; Zhang, F.; Gong, H.; Wei, F.; Zhuang, J.; Karshalev, E.; Esteban-Fernández de Avila, B.; Huang, C.; Zhou, Z.; Li, Z.; Yin, L.; Dong, H.; Fang, R. H.; Zhang, X.; Zhang, L.; Wang, J. Enzyme-powered Janus platelet cell robots for active and targeted drug delivery. *J. Sci. Robot.* **2020**, *5*, No. eaba6137.
(47) Ha, L.; Choi, K. M.; Kim, D.-P. Interwoven MOF-Coated Cells as a Novel Carrier of Toxic Proteins. *ACS Appl. Mater. Interfaces* **2021**, *13*, 18545−18553.

https://doi.org/10.1021/acsbiomaterials.1c00539
ACS Biomater. Sci. Eng. XXXX, XXX, XXX−XXX